Articles

Anticooperativity in a Glu−Lys−Glu Salt Bridge Triplet in an Isolated α-Helical Peptide†

Teuku M. Iqbalsyah and Andrew J. Doig*

Faculty of Life Sciences, Jackson's Mill, The University of Manchester, P.O. Box 88, Sackville Street, Manchester M60 1QD, U.K.

Received May 11, 2005; Revised Manuscript Received June 16, 2005

ABSTRACT: Salt bridges between oppositely charged side chains are well-known to stabilize protein structure, though their contributions vary considerably. Here we study Glu−Lys and Lys−Glu salt bridges, formed when the residues are spaced *i*, *i* + 4 surface of an isolated α-helix in aqueous solution. Both are stabilizing by −0.60 and −1.02 kcal/mol, respectively, when the interacting residues are fully charged. When the side chains are spaced *i*, *i* + 4, *i* + 8, forming a Glu−Lys−Glu triplet, the second salt bridge provides no additional stabilization to the helix. We attribute this to the inability of the central Lys to form two salt bridges simultaneously. Analysis of these salt bridges in protein structures shows that the Lys−Glu interaction is dominant, with the side chains of the Glu−Lys pair far apart.

Proteins are stabilized most commonly by hydrogen bonds, van der Waals packing, and hydrophobic and electrostatic interactions. The amino acid side chains interact within a complex network of multiple noncovalent bonds, which may reinforce or weaken each other. Salt bridge interactions, in particular, are found in ∼60% of protein structures. One-third of the charged amino acids participating in salt bridge formation are found as complex salt bridges (with three or more amino acids), where triplet salt bridges are the most abundant. Approximately 20% of the total salt bridges found in proteins reside in α-helix secondary structure in either an *i*, *i* + 3 or an *i*, *i* + 4 spacing (*1*).

The energetic role of salt bridges in protein structure stability has been found to vary. Solvent-exposed salt bridges contribute only marginally to protein stability (*2*−*4*). In contrast, a buried salt bridge stabilizes the native state by up to 5 kcal/mol (*5*, *6*). Theoretical studies of solvation suggest that internal or external salt bridges contribute only marginally to protein stability, because of the high-energy penalty of desolvating ions within the interior or near the surface of a protein, thus diminishing the expected gain in strength of ionic interactions (*7*). The strength of salt bridges has been found to be determined by several factors: (a) the geometry and distance of the interactions (*8*), (b) the degree of exposure to solvent (*9*), and (c) the effect of neighboring residues (*10*). The frequency of salt bridges in proteins from thermophilic proteins is high, suggesting an association with increased protein stability (*11*, *12*).

Many attempts have been made to evaluate the strength of multiple salt bridges, particularly in proteins. A coupling interaction of an Asp8−Arg110−Asp12 triplet on the surface of barnase stabilizes the triplet by 0.8 kcal/mol relative to the sum of isolated pairs (*4*). A salt bridge and a hydrogen bond in an Asp14−Ser77−Arg17 triplet in the λ repressor are stabilizing by 1.5 and 0.8 kcal/mol, respectively (*13*). Kallenbach and co-workers reported that a GCN4 leucine zipper is stabilized by 1.7 kcal/mol upon introduction of an Arg−Glu−Arg triplet at the helix surface (*2*). The presence of many additional side chains close to the sites of interest, however, complicates the generalization of the energetic role of the salt bridge network in proteins. For this reason, we have studied a simple salt bridge network in a more isolated environment, i.e., in a short peptide.

The first evaluation of the strength of an engineered complex salt bridge in a peptide was reported by Mayne et al. (*14*) after studying a multiple-salt bridge involving Glu3, Asp4, and Arg7 in an 11-mer α-helix. The triplet contributes substantially to the α-helix stability with a Δ*G* of −1.2 kcal/mol. A triplet of charged Arg−Glu−Arg residues spaced *i*, *i* + 4, *i* + 8 or *i*, *i* + 3, *i* + 6 also stabilizes α-helical peptides by −1.5 or −1.0 kcal/mol, respectively, which is more than the additive contribution of two single salt bridges (*15*). A similar stabilizing effect in an Arg−Phe−Met triplet in *i*, *i* + 4, *i* + 8 spacing was also observed, although the triplet is not a complex salt bridge (*16*). Other non-salt bridge triplets in isolated helical peptides have also been reported, for example, Glu−Phe−Arg (*17*) and Glu−Phe−Glu (*18*), although they do not show significant effects on peptide stability.

† T.M.I. is supported by a TPSDP scholarship from the Ministry of National Education of the Government of Indonesia.

* To whom correspondence should be addressed: Faculty of Life Sciences, Jackson's Mill, The University of Manchester, P.O. Box 88, Sackville Street, Manchester M60 1QD, U.K. Phone: +44-(161) 200 4224. Fax: +44(161) 236 0409. E-mail: andrew.doig@manchester.ac.uk.

10.1021/bi0508690 CCC: $30.25
Published on Web 07/15/2005

Most triplet salt bridges studied so far were found to be cooperative; i.e., the free energy of the pairs present simultaneously is greater than the sum of the individual pairs. It is thus interesting to study a triplet salt bridge in an isolated α-helix having the opposite effect. In this study, we examine Glu−Lys−Glu interactions when present simultaneously in an *i*, *i* + 4, *i* + 8 spacing. The free energies of Glu−Lys and Lys−Glu interactions spaced *i*, *i* + 4 in isolated α-helical peptides have previously been found to be stabilizing by approximately −0.4kcal/mol in both orientations (*19*). In a Glu−Lys−Glu triplet, the central Lys side chain cannot point toward both Glu side chains simultaneously. The Glu−Lys−Glu triplet may therefore be less stabilizing than the sum of the two individual interactions, giving rise to anticooperativity. We have recently demonstrated that strong cooperativity in Arg−Phe−Met triplets can be attributed to a shared preference for the trans rotamer in the central Phe. The energetic cost of restricting the Phe residue is only paid once in the triplet, rather than twice when the interactions are separate (*16*). We consider whether rotamer preferences can also help explain the energetics of the Glu−Lys−Glu triplet.

MATERIALS AND METHODS

Peptide Synthesis. Peptides were synthesized by the solid-phase method on an Applied Biosystems 433A peptide synthesizer on a 0.1 mmol scale using Fmoc (9-fluorenylmethoxycarbonyl) chemistry. C-Terminal amides were made using Rink amide resin (CN Biosciences). N-Termini were acetylated with a 4% (v/v) acetic anhydride/5% (v/v) pyridine dimethylformamide mixture for 30 min at room temperature. Peptides were cleaved from the resin using a mixture of 95% trifluoroacetic acid, 2.5% triisopropylsilane, and 2.5% water.

Peptides were purified by C_{18} reverse-phase HPLC, and their molecular weights were checked by MALDI mass spectrometry. Final purity was checked by analytical C_{18} HPLC. Peptide concentration was determined by measuring the tyrosine UV absorbance of aliquots of a stock solution dissolved in water using an ϵ_{275} of 1450 M^{-1} cm^{-1} (*20*).

Circular Dichroism Measurements. The secondary structure of each peptide was checked using circular dichroism between 190 and 250 nm. Equilibrium CD measurements for α-helical structure were made at 222 nm with a Jasco J810 spectropolarimeter at 273 K. Ellipticity was measured in 10 mM NaCl and 5 mM sodium phosphate at pH 2.9 and 8.2. CD data in millidegrees were converted to mean residue ellipticity using the relation $[\theta]_{222} = \theta/(\text{molar concentration} \times 18 \text{ residues} \times 10)$, in degrees square centimeter per decimole. Helix content was calculated as $[\theta]_{222(\text{observed})}/[\theta]_{222(\text{max})}$. $[\theta]_{222(\text{max})}$ is given by $-40000(1 - 2.5/N)$, where N is the number of amino acids in the peptide (*21*).

pH titrations were performed in a 3 mL 1.0 cm path length quartz cell at 273 K. The buffer used for pH titrations contained 10 mM NaCl, 1 mM sodium phosphate, 1 mM sodium borate, and 1 mM sodium citrate. The pH meter was calibrated for measurements at 273 K. The pH was adjusted during the titrations with aliquots of dilute HCl or NaOH. The volume of HCl or NaOH added was used for concentration correction.

Depending on the number of apparent titratable groups in the curve, the ellipticity data from the titrations were fitted to a Henderson−Hasselbach equation. For one apparent pK_a, $[\theta]_{222}$ as a function of pH is given by

$$[\theta]_{222} = [\theta]_{222,\text{high}-\text{pH}}\left(1 - \frac{1}{1 + 10^{\text{pH}-\text{p}K_a}}\right) + [\theta]_{222,\text{low}-\text{pH}}\left(\frac{1}{1 + 10^{\text{pH}-\text{p}K_a}}\right)$$

where $[\theta]_{222,\text{high}-\text{pH}}$ and $[\theta]_{222,\text{low}-\text{pH}}$ are the molar ellipticities measured at 222 nm at the titration end points at high and low pH, respectively.

The equation for two different pK_a's is given by

$$[\theta]_{222} = [\theta]_{222,\text{mid}-\text{pH}}\left(1 - \frac{1}{1 + 10^{\text{pH}-\text{p}K_{a1}}}\right) + [\theta]_{222,\text{low}-\text{pH}}\left(\frac{1}{1 + 10^{\text{pH}-\text{p}K_{a1}}}\right) + [\theta]_{222,(\text{mid}-\text{pH}-\text{high}-\text{pH})}\left(1 - \frac{1}{1 + 10^{\text{pH}-\text{p}K_{a2}}}\right)$$

where pK_{a1} and pK_{a2} are the pK_a's measured for the acid−base equilibrium at low and high pH, respectively. $[\theta]_{222,\text{high}-\text{pH}}$, $[\theta]_{222,\text{mid}-\text{pH}}$, and $[\theta]_{222,\text{low}-\text{pH}}$ are the molar ellipticities measured at 222 nm at the titration end points at high, intermediate, and low pH, respectively. $[\theta]_{222,\text{mid}-\text{pH}-\text{high}-\text{pH}}$ is the change in molar ellipticity associated with pK_{a2}.

Fitting of Helix−Coil Parameters for Side Chain−Side Chain Interactions (p values). A simplified explanation of *p* values in helix−coil theory is as follows. Lifson−Roig-based models (*22*) describe the helix−coil transition as a two-state model on the level of individual amino acids, as either *h* (helix) or *c* (coil) according to its backbone dihedral angles (ψ and ϕ). Each residue in a helical sequence has a nonunity statistical weight based upon its own state and the states of the neighboring residues. The model now considers not only the original nucleating (v) and propagating parameters (w) but also N-capping (n) and C-capping (c), N1 (n_1), N2 (n_2w), N3 (n_3w), and side chain−side chain interactions (for review, see ref *23*). When an *i*, *i* + 4 interaction occurs between the residues at both ends of a helical *hhhhh* stretch, the residue in the middle of the quintet is mathematically assigned weight *pw*. The *p* value shows how the weight for forming the helical stretch is perturbed by the side chain interaction across the quintet. It can then be used to calculate the free energy of interaction as $\Delta G_{(i,i+4)} = -RT \ln p$ (*24*). The *p* values for the *i*, *i* + 4 side chain−side chain interactions were determined using a modified Lifson−Roig-based helix−coil theory, implemented in Scint2 (*24*). The inputs to the program are the peptide sequences and corresponding experimental helix contents, a library of *w*, *n*-cap, *c*-cap, and v^2 values for each amino acid, an *n*-cap value for acetyl and a *c*-cap value for amide (*25*), and a library of *i*, *i* + 4 interactions. The *p* values for EK and KE *i*, *i* + 4 interactions were calculated from the interaction free energies of Smith and Scholtz (*19*) as $\Delta G = -RT \ln p$. Values used for side chain *i*, *i* + 4 interactions for E^-K^+ and K^+E^- were 2.15 and 2.09, respectively, and for $E^\circ K^+$ and K^+E° were 1.50 and 1.45, respectively. When the *p* values needed refitting, parameters were varied until they converged on essentially unchanging values in agreement with experimental helicities.

Table 1: Peptides Used To Measure EKE Triplet Interactions

peptide	sequence	predicted helicity[a] (%) parameter values of E^- and K^+ [b]	predicted helicity[a] (%) parameter values of E° and K^+ [c]	experimental helicity (%) pH 8.2	experimental helicity (%) pH 2.9
E5K5E	Ac-AAA**E**AAAA**K**AAAA**E**AKGY-NH_2	50	57	51	56
E5K4E	Ac-AAA**E**AAAA**K**AAA**E**AKAGY-NH_2	56	59	67	65
E4K5E	Ac-AAAA**E**AAA**K**AAAA**E**AKGY-NH_2	59	61	63	63
E4K4E	Ac-AAAA**E**AAA**K**AAA**E**AKAGY-NH_2	64	63	60	61

[a] Predicted using Scint2. Parameter values of *n*, *v*, *w*, and *c* were taken from ref *25*. [b] *p* values for E^-K^+ and K^+E^- were 2.15 and 2.09, respectively (*19*). [c] *p* values for E°K^+ and K^+E° were 1.50 and 1.45, respectively (*19*).

Database Search. A survey was conducted on a data set obtained from a set of crystal structures in the ASTRAL database (SCOP 1.63 Sequence Resources) (*26*), which is based on domains rather than entire structures. Each domain in the data set represents one superfamily and is the member of that superfamily with the best SPACI score. The SPACI score is a measure of the reliability and precision of a crystallographically determined structure in a PDB file. The data set contained 1135 chains with a total of 195 875 amino acid residues, and there was less than 20% sequence identity between any pair. These were processed using the DSSP algorithm to give secondary structure information as implemented in SSTRUC (*27*).

First, the data set was probed for helices of at least five helical residues (*hhhhh*) for pairwise *i*, *i* + 4 EK and KE interactions. EK and KE were categorized as pairs in coil when they, and the three intervening residues, were not all in helical conformations. A Glu−Lys−Glu helical triplet requires at least nine consecutive helical residues for *i*, *i* + 4, *i* + 8 interactions to be present. The rotamer χ_1 and χ_2 preferences for Glu and Lys residues were then determined. Definitions of χ_1 and χ_2 rotamer angles for an sp^3-sp^3 bond are as follows: gauche$^+$ (g^+) $\chi_1 = -60 \pm 60°$, trans (*t*) $\chi_1 = 180 \pm 60°$, and gauche$^-$ (g^-) $\chi_1 = 60 \pm 60°$.

The frequencies and errors were further calculated according to the following equations (*28*):

$$p_i = n_i/N$$

where n_i is the number of occurrences in *N* observations

$$\sigma p_i = [p_i(1 - p_i)/N]^{0.5}$$

where σp_i is the standard deviation in p_i.

RESULTS

Peptide Design. A series of intrinsically helical alanine-based peptides with different spacing of the interacting residues was designed to allow the quantitative evaluation of the role of Glu−Lys−Glu triplets in helix stability (Table 1). E5K5E was the control peptide in the EKE series. The Lys−Glu *i*, *i* + 4 interaction was achieved by swapping Ala at N5 with Glu at N4. Similarly, the Glu−Lys *i*, *i* + 4 interaction was achieved by changing AEAK to EAKA. An Ala residue was placed between Glu and Lys to avoid any close-range charge effects. The *i*, *i* + 2 spacing ensures the residues are on opposite faces of the helix. Shorter helices that could be made by moving Glu toward the N-terminus were prevented because Glu has unique preferences to be at N1 (*29*), N2 (*30*), or N3 (*31*). The helicity would be perturbed by Glu interacting with free amide NH groups at N1, N2, and N3, as well as with the helix macro dipole at the N-terminus.

Gly is a helix breaker and was placed between Tyr and the rest of the sequence to prevent Tyr perturbation on the circular dichroism signal (*32*). Tyr was introduced at the C-terminus to allow the concentrations of the peptides to be determined. The N- and C-termini were blocked with an acetyl group and an amide group, respectively, minimizing the destabilizing interactions that may occur with the charged termini. This also creates an extra hydrogen bond at each terminus. Acetyl groups also substantially stabilize the helix (*33*).

All peptides were monomeric between 5 and 100 μM as shown by invariance of CD molar ellipticity with concentration (data not shown). E4K4E, however, showed a change in secondary structure from entirely helical to a mixture of helix and β-sheet when left for a prolonged time (>48 h). This was observed by running analytical HPLC followed by MS analysis on the peptide after incubation for 48 h. HPLC analysis showed a tailing in the pure E4K4E peak, but both species gave identical masses when checked by MALDI. The CD spectra in range of 190−250 nm showed a conformational shift from α-helix to β-sheet (data not shown). Data on the E4K4E peptide were thus collected solely on freshly dissolved pure lyophilized peptide. The reason behind the delayed aggregation could be that the E4K4E peptide contains residues assisting solubilization (two Glu and three Lys residues) distributed on only one face of the helix. Two, if not three, of the residues are also involved in side chain interactions.

Refitting p Values. The Glu−Lys pair has previously been studied for different spacings and orientations in isolated α-helices (*19*, *34*). The stabilizing effect of EK and KE did not vary significantly with orientation. We found dissimilar results, however, with Lys *i* and Glu *i* + 4 more stabilizing than Glu *i* and Lys *i* + 4. The ellipticities of all EKE peptides were invariant and within error at three different salt concentrations, 0.01, 1.0, and 2.5 M NaCl (data not shown). This suggests that the interaction at high salt is not just a simple electrostatic interaction as the major component of the interaction between Glu and Lys cannot be screened by external salts. Hydrogen bonding thus provides the major part of the stabilizing effect in the EK and KE pairs, as proposed previously by Scholtz et al. (*34*).

The helicities of the EKE series peptides were measured at a range of pH values (Table 1). The terms E and B in ExKyE and BxKyB stand for Glu$^-$ and Glu°, respectively. The control peptides E5K5E and B5K5B show an excellent agreement between predicted and experimental helicity, indicating that errors in previous parameter values used in

Table 2: Energetics of Interaction in EKE Peptides

interaction	refitted *p* value (±3% helicity error)	$\Delta G_{(i,i+4)}$ (kcal/mol)[a]	multiplication factor (mf) (±3% helicity error)	refitted *p* values × mf in triplet (±3% helicity error)	ΔG anticooperativity (kcal/mol)[b]
KE	6.6 (4.4−11.7)	−1.02 (−0.81 to −1.33)		2.6 (1.5−5.2)	
EK	3.0 (2.2−4.5)	−0.60 (−0.43 to −0.81)		1.2 (0.8−2.0)	
EKE		−1.62[c] (−1.24 to −2.15)	0.39 (0.34−0.45)		1.02 (0.87−1.16)
KB[d]	2.5 (1.9−3.6)	−0.50 (−0.35 to −0.69)		1.6 (1.1−2.6)	
BK[d]	1.7 (1.3−2.4)	−0.29 (−0.13 to −0.47)		1.1 (0.7−1.8)	
BKB[d]		−0.79[c] (−0.48 to −1.16)	0.65 (0.57−0.74)		0.47 (0.33−0.60)

[a] Calculated as $-RT \ln p$ using refitted *p* values in column 2. [b] Calculated as $-RT \ln(\text{mf})^2$. [c] Additive ΔG of the individual pairs. [d] B represents Glu°.

the prediction for residues in the sequences are low and that the helix−coil theory that is used is accurate. The controls thus provide an independent system for measuring the preferred interactions. There are, however, disagreements between predicted and experimental helicities when *i*, *i* + 4 interactions are present, particularly for the KE−KB orientation. The sequences of peptides previously used to obtain the *p* values for EK−BK and KE−KB interactions are Ac-AAQAAEAQAKAAQAAY-NH_2 and Ac-AAQAAKAQAE-AAQAAY-NH_2, respectively (*19*). The Gln residues near the helix termini in these peptides may interact with Glu and Lys in an *i*, *i* + 3 fashion that could give errors in the estimation of the interaction energies. Our peptides do not contain these *i*, *i* + 3 interactions. In addition, Gln could form a significant interaction at the N3 position with the peptide backbone (*31*).

The original *p* values of the E^-K^+ (2.15), K^+E^- (2.09), $E°K^+$ (1.50), and $K^+E°$ (1.45) *i*, *i* + 4 interactions were thus refitted individually by varying them until the calculated helicity agreed with experiment. Refitting *p* values for E^-K^+ and K^+E^- gives values of 3.0 and 6.6, respectively, equivalent to −0.60 and −1.02 kcal/mol, respectively, giving an additive ΔG of −1.62 kcal/mol. Refitting *p* values for $E°K^+$ and $K^+E°$ gives values of 1.7 and 2.5, respectively, corresponding to −0.29 and −0.50 kcal/mol, respectively, giving an additive ΔG of −0.79 kcal/mol (Table 2).

Using the refitted values, the predicted helicities are 74 and 69% for the corresponding E4K4E and B4K4B peptides, respectively. These predictions are significantly higher than the experimental helicities of 60 and 61% for E4K4E and B4K4B, respectively. These large differences prove qualitatively that there is a large destabilizing effect as a result of pairwise coupling in the E4K4E and B4K4B peptides. This is clear from the raw data, where there is remarkably a decrease in helix content in E4K4E compared to E5K4E and E4K5E, despite the introduction of an additional salt bridge.

For the predicted helicity to agree with experiment in the E4K4E−B4K4B peptides, the *p* value of each pair was decreased by multiplication factors (mf) of 0.39 and 0.65 for E4K4E and B4K4B, respectively (Figure 1). This decreases the statistical weight of all conformations within nine consecutive helical residues from Glu_{N-term} to Glu_{C-term} simultaneously by $(\text{mf})^2$. The *p* values for E^-K^+ and K^+E^- in the E4K4E peptide become 1.2 and 2.6, respectively, equivalent to −0.09 and −0.51 kcal/mol, respectively. The *p* values for $E°K^+$ and $K^+E°$ in the B4K4B peptide became 1.1 and 1.6, respectively, equivalent to −0.05 and −0.26 kcal/mol, respectively.

The free energy resulting from the EK and KE coupling was calculated as $-RT \ln(\text{mf})^2$, giving ΔG values of 1.0 kcal/mol (0.9−1.2 kcal/mol) and 0.5 kcal/mol (0.3−0.6 kcal/mol) for E4K4E and B4K4B, respectively. These values show an anticooperativity effect in the triplet as they are positive, making the ΔG in the triplets smaller than the sum of the energies of the individual interactions. The error in *p* was calculated by repeating the fitting procedure using experi-

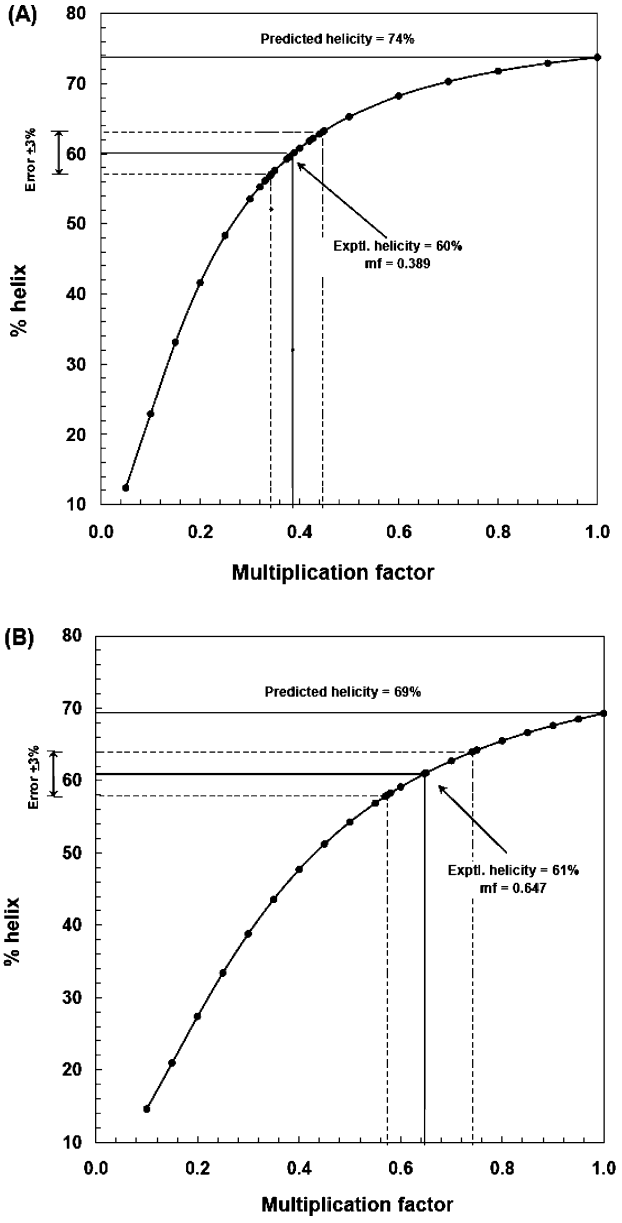

FIGURE 1: Adjustment of *p* values for pairs when present simultaneously in the triplet so that predicted helicity agrees with experiment: (A) E^-K^+ and K^+E^- pairs in the EKE triplet and (B) $E°K^+$ and $K^+E°$ pairs in the BKB triplet.

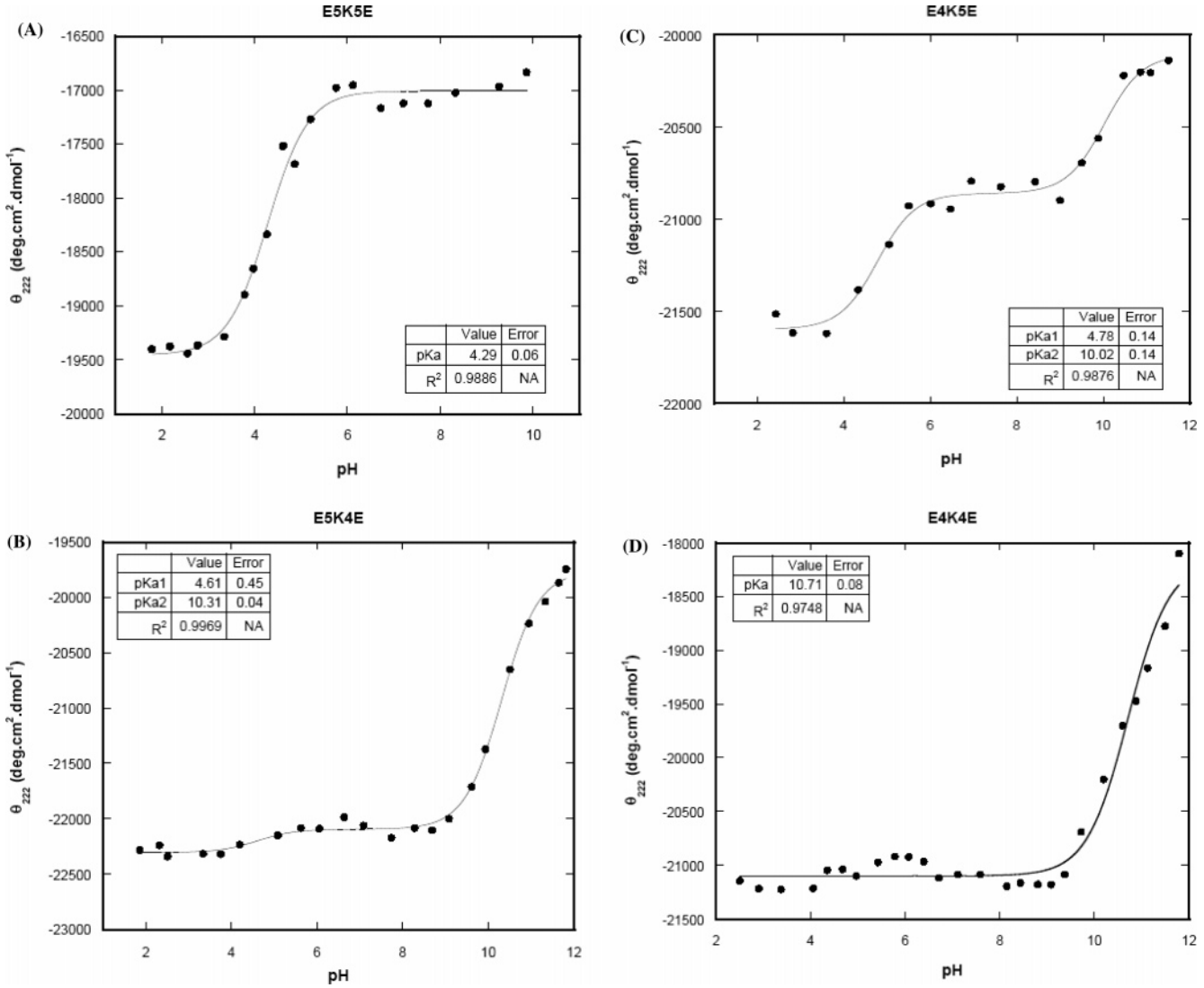

FIGURE 2: pH titration of EKE peptides: (A) E5K5E, (B) E4K5E, (C) E5K4E, and (D) E4K4E.

mental helicities increased or decreased by 3% to account for experimental error in the measurements of helicity.

pH Titrations of EKE Peptides. The helicities of the EKE peptides were followed as a function of pH using far-UV CD (Figure 2). pK_a values for the ionizable side chain groups were evaluated between approximately pH 2 and 11 by curve fitting the CD data to the Henderson−Hasselbach equations (see Materials and Methods). The upper range of accessible pH is given by Lys deprotonation, which leads to peptide aggregation.

The pK_a values of the two Glu residues in E5K5E cannot be separated. Only one observable transition across the pH range is present as the pK_a values of the two Glu residues are similar. The pK_a of 4.29 ± 0.06 is comparable to the pK_a value of Glu of 4.5 in a model compound *N*-acetyl acid amide (*35*). The unperturbed pK_a value for Glu residues is reasonable, as the side chains are not involved in any interactions, yet the helix content is strongly influenced by the ionization state. Protonation of Glu residues increases the helix content of E5K5E by ~7%. Previous work has found that helix propagation parameters of a single Glu in the helix interior give a difference in energy between protonated and unprotonated Glu of 0.15 kcal/mol (*25*, *34*).

Only one Glu transition was observed in the E4K5E and E5K4E peptides. The pK_a values for E4K5E and E5K4E are 4.78 ± 0.14 and 4.61 ± 0.45, respectively. It was expected that one of the Glu residues would have had a different pK_a value as it interacts with Lys. The difference in ellipticities upon protonation is very small, making it difficult to fit the data for calculation of the pK_a values, however. When the interaction is present, the destabilizing effect of having a charged Glu in the helix is weakened, which is exhibited by the low ellipticity difference between charged and uncharged Glu. The pK_a values in E4K5E and E5K4E surprisingly appear to be shifted to higher values than in E5K5E, though the experimental errors in the pK_a values make this conclusion uncertain. A decrease in Glu pK_a would be expected within a salt bridge, as the nearby positive charge would favor Glu^-. The transition above pH 10 can be attributed to protonation of Tyr.

The titration curve of the E4K4E peptide may have a weak transition between pH 4 and 6, similar to that observed in Figure 2B, though this is difficult to identify as the putative change in θ_{222} is very small. Repeating the titration three times did not convincingly show that this transition was real. Data fitting when using equations for two or three apparent pK_a values gave large errors of up to two pH units in the

Table 3: χ_1 Rotamer Population of Glu and Lys in α-Helices

residue	rotamer distribution[a] g^-	t	g^+	no. of observations
Glu	0.04 ± 0.003[b]	0.39 ± 0.01	0.57 ± 0.01	5947
Lys	0.03 ± 0.003	0.44 ± 0.01	0.53 ± 0.01	4409
Glu in Glu−Lys pair[c]	0.05 ± 0.01	0.47 ± 0.02	0.48 ± 0.02	468
Lys in Glu−Lys pair[c]	0.02 ± 0.01	0.37 ± 0.02	0.61 ± 0.02	468
Lys in Lys−Glu pair[c]	0.02 ± 0.01	0.62 ± 0.02	0.36 ± 0.02	411
Glu in Lys−Glu pair[c]	0.03 ± 0.01	0.27 ± 0.02	0.70 ± 0.02	411

[a] Data were from a domain search of 1135 nonredundant proteins containing 4778 helices with a total of 65 472 residues in the ASTRAL database (SCOP 1.63 Sequence Resources). Rotamer definitions: g^+ when $-120° < \chi_1 < 0°$, g^- when $0° < \chi_1 < 120°$, and t when $-120° < \chi_1 < 240°$. [b] Errors were calculated as $\sigma p_i = [p_i(1 - p_i)/N_i]^{1/2}$, where p_i is the rotamer population and N_i is the total number of observations. [c] The pairs were observed in *hhhhh* conformations.

pK_a values. The data were therefore fitted using the equation for one apparent pK_a. In general, the θ_{222} does not significantly vary from pH 2 to 9, showing that the helix content of the peptide does not change when either Glu side chain is protonated. This is due to a decrease in helix content when Glu is deprotonated, as Glu^- has a weaker helix preference than Glu°, which is counteracted by stronger salt bridges with Glu^- in the helix. These two effects are close to equal and opposite in sign, giving no net change in θ_{222}.

Rotamer Distributions of Glu and Lys Residues. We have previously demonstrated that rotamer preference was helpful in explaining cooperativity in an RFM triplet in an α-helical peptide (*16*). This triplet only needs to pay the cost of restricting the central Phe residue into a trans conformation once, rather than twice when the interactions are separate. We therefore examined the χ_1 rotamer preferences of Glu and Lys. This PDB-derived rotamer analysis is based on the assumption that the rotamer distributions determined in the presence of tertiary contacts in proteins can be applied to peptides. We only analyze the χ_1 rotamer as χ_2 is predominantly in the *t* rotamer in all cases.

χ_1 Rotamer Preference of Glu and Lys. As summarized in Table 3, the Glu χ_1 population in an EK pair is spread almost equally between g^+ (48%) and *t* (47%). The Lys χ_1 tends to be in g^+ (61%). In the KE pair, the Lys χ_1 favors the *t* rotamer (61%). The Glu χ_1 is overwhelmingly in g^+. Individual Glu and Lys rotamer preferences in the helix were included for comparison.

χ_1 Rotamer Preference of Glu and Lys in the EKE Triplet. We found 58 helices containing the EKE triplet spaced *i*, *i* + 4, *i* + 8 in our data set (Table 4). This number is not large, making quantitative conclusions about rotamer preferences in the triplet difficult. Almost half the χ_1 rotamer combinations were g^+, *t*, g^+ for the corresponding Glu, Lys, and Glu residues in the EKE triplet, while one-fifth were in a g^+, g^+, g^+ combination. This suggests that the N-terminal Glu in the EK pair switches from equally χ_1 g^+ (48%) and *t* (47%) to mostly g^+ when in the EKE triplet. The Lys χ_1 also switches from mostly g^+ (61%) to *t* in the triplet. The Glu and Lys χ_1 preference in the KE pair seems to be retained in the triplet. The majority of Lys χ_1 in the EKE triplet adopt the *t* conformation, as for Lys in the KE pair. The preference of Glu χ_1 g^+ in the EKE triplet is also comparable to that of Glu χ_1 g^+ in the KE pair. Overall, this suggests that within the EKE triplet, the KE interaction is present, while the EK interaction is not. The central Lys cannot adopt the preferred rotamers for both salt bridges simultaneously.

Table 4: χ_1 Rotamer Distribution of the Interacting Residues in the Glu−Lys−Glu Triplet in *i*, *i* + 4, *i* + 8 Spacing

χ_1 rotamer combination[a] Glu	Lys	Glu	total no. observed in the *hhhhhhhhh* conformation	%
g^+	g^-	g^+	1	2
g^-	g^+	g^-	1	2
g^+	g^+	g^+	12	21
t	g^+	*t*	5	9
g^+	not defined	g^+	1	2
g^-	*t*	g^-	2	3
g^+	*t*	g^+	27	47
t	*t*	*t*	9	16
total			58	100

[a] Data were from a domain search of 1135 nonredundant proteins containing 4778 helices with a total of 65 472 residues in the ASTRAL database (SCOP 1.63 Sequence Resources). Rotamer definitions: g^+ when $-120° < \chi_1 < 0°$, g^- when $0° < \chi_1 < 120°$, and *t* when $-120° < \chi_1 < 240°$.

Our rotamer analysis contradicts the previous finding that the geometry of the interactions between acidic and basic residues is very similar in simple and complex salt bridges (*1*). The authors proposed that adding one residue to a simple interaction shows a minor change in geometry, in terms of atomic distance, partly because half of the salt bridge interaction is already constrained in a geometry that satisfies a complex salt bridge. The KE pair is indeed constrained, but the rotamer preferences in EK pairs change when in the triplet. Examples of triplet interactions are shown in Figure 3. Figure 3C shows a typical example of an EKE triplet, showing how the KE interaction dominates, confirming the rotamer analysis above, and that essentially only a single salt bridge is present.

DISCUSSION

The salt bridges in the α-helical peptides studied here are solvent-exposed and in isolation from interactions with neighboring residues. The EKE series peptides are a useful model for studying solvent-exposed salt bridges as they simplify the energetic role of the interacting pairs. The E4K5E peptide has a lower helix content than E5K4E, suggesting that the EK interaction is weaker than that of KE. This is confirmed by helix−coil theory analysis, which gives free energies of −1.02 and −0.60 kcal/mol for KE and EK, respectively, and by structural analysis of triplets. When the EKE triplet is present, KE dominates so the Lys predominantly adopts the rotamer that points it toward the *i* + 4 Glu (Figure 3C). Previously reported ΔG values show that the stabilizing free energies for EK and KE pairs are fairly

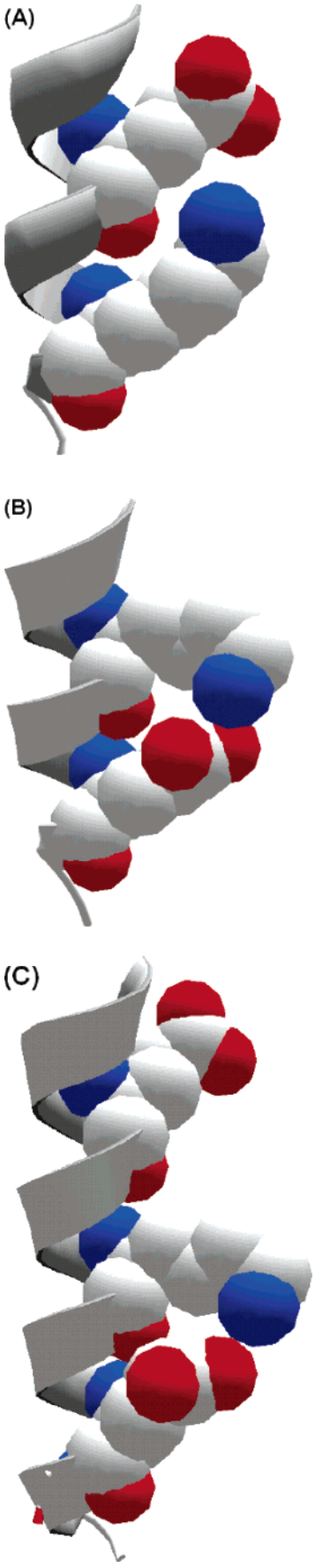

FIGURE 3: Examples of structure: (A) EK interaction between Glu62 and Lys66 in PDB entry 1A48, (B) KE interaction between Lys175 and Glu179 in PDB entry 1AOP, and (C) EKE interaction involving Glu110, Lys114, and Glu118 in PDB entry 1L2P.

similar (*19*, *34*), contradicting the findings in this study. It appears that in the E4K4E peptide the Lys can interact with only one of the Glu residues. Thus, when we compare E4K4E to E5K4E, the addition of the second Glu−Lys salt bridge has little stabilizing effect. In fact, there is a slight decrease in stability that can be attributed to moving a Glu further from the N-terminus of the peptide, weakening any helix−dipole interactions. Glu is a strongly favored residue at the N1, N2, and N3 positions, which it can populate if the helix frays. The lower helicity in E4K4E compared to E4K5E is more difficult to explain. We suggest that when this change is made, the Lys moves to form a KE interaction, rather than the weaker EK in E4K5E. In addition, the Glu is moved further from the C-terminus, where it will form a destabilizing interaction with the helix dipole. The combination of these three effects, which are difficult to separate, results in a small decrease in helix content.

CONCLUSIONS

Variations in the strength of salt bridges have been noted before and attributed to solvation effects. On the surface of a helical peptide, changes in solvation are minor, however. We have shown that the addition of a salt bridge can be worth essentially nothing. We attribute this to the inability of the central Lys to form two interactions simultaneously. Even in the simplest systems, noncovalent interactions are nonadditive and can be cooperative or anticooperative, depending on how compatible the conformational preferences of the interactions are. Rotamer analysis is useful in rationalizing these effects.

ACKNOWLEDGMENT

The Michael Barber Mass Spectrometry Facility at The University of Manchester is thanked for verifying peptide identity. We thank Neil Errington for helpful assistance with database searches.

REFERENCES

1. Musafia, B., Buchner, V., and Arad, D. (1995) Complex salt bridges in proteins: Statistical analysis of structure and function, *J. Mol. Biol. 254*, 761−770.
2. Spek, E. J., Bui, A. H., Lu, M., and Kallenbach, N. R. (1998) Surface salt bridges stabilize the GCN4 leucine zipper, *Protein Sci. 7*, 2431−2437.
3. Daopin, S., Sauer, U., Nicholson, H., and Matthews, B. W. (1991) Contributions of engineered surface salt bridges to the stability of T4 lysozyme determined by directed mutagenesis, *Biochemistry 30*, 7142−7153.
4. Horovitz, A., Serrano, L., Avron, B., Bycroft, M., and Fersht, A. R. (1990) Strength and co-operativity of contributions of surface salt bridges to protein stability, *J. Mol. Biol. 216*, 1031−1044.
5. Anderson, D. E., Becktel, W. J., and Dahlquist, F. W. (1990) pH-induced denaturation of proteins: A single salt bridge contributes 3−5 kcal/mol to the free energy of folding of T4 lysozyme, *Biochemistry 29*, 2403−2408.
6. Tissot, A. C., Vuilleumier, S., and Fersht, A. R. (1996) Importance of two buried salt bridges in the stability and folding pathway of Barnase, *Biochemistry 35*, 6786−6794.
7. Hendsch, Z. S., and Tidor, B. (1994) Do salt bridges stabilize proteins? A continuum electrostatic analysis, *Protein Sci. 3*, 211−226.
8. Kumar, S., and Nussinov, R. (2002) Relationship between ion pair geometries and electrostatic strengths in proteins, *Biophys. J. 83*, 1595−1612.
9. Takano, K., Tsuchimori, K., Yamagata, Y., and Yutani, K. (2000) Contribution of salt bridges near the surface of a protein to the conformational stability, *Biochemistry 39*, 12375−12381.

10. Makhatadze, G. I., Loladze, V. V., Ermolenko, D. N., Chen, X. F., and Thomas, S. T. (2003) Contribution of surface salt bridges to protein stability: Guidelines for protein engineering, *J. Mol. Biol. 327*, 1135−1148.
11. Elcock, A. H. (1998) The stability of salt bridges at high temperatures: Implications for hyperthermophilic proteins, *J. Mol. Biol. 284*, 489−502.
12. Kumar, S., Ma, B. Y., Tsai, C. J., and Nussinov, R. (2000) Electrostatic strengths of salt bridges in thermophilic and mesophilic glutamate dehydrogenase monomers, *Proteins 38*, 368−383.
13. Marqusee, S., and Sauer, R. T. (1994) Contributions of a hydrogen bond/salt bridge network to the stability of secondary and tertiary structure in λ repressor, *Protein Sci. 3*, 2217−2225.
14. Mayne, L., Englander, S. W., Qiu, R., Yang, J. X., Gong, Y. X., Spek, E. J., and Kallenbach, N. R. (1998) Stabilizing effect of a multiple salt bridge in a prenucleated peptide, *J. Am. Chem. Soc. 120*, 10643−10645.
15. Olson, C. A., Spek, E. J., Shi, Z. S., Vologodskii, A., and Kallenbach, N. R. (2001) Cooperative helix stabilization by complex Arg-Glu salt bridges, *Proteins 44*, 123−132.
16. Iqbalsyah, T. M., and Doig, A. J. (2005) Pairwise coupling in an Arg-Phe-Met triplet stabilizes α-helical peptide via shared rotamer preferences, *J. Am. Chem. Soc. 127*, 5002−5003.
17. Shi, Z. S., Olson, C. A., and Kallenbach, N. R. (2002) Cation-π interaction in model α-helical peptides, *J. Am. Chem. Soc. 124*, 3284−3291.
18. Shi, Z., Olson, C. A., Bell, A. J., and Kallenbach, N. R. (2002) Non-classical helix-stabilizing interactions: C−H···O H-bonding between Phe and Glu side chains in α-helical peptides, *Biophys. Chem. 101*−*102*, 267−279.
19. Smith, J. S., and Scholtz, J. M. (1998) Energetics of polar side-chain interactions in helical peptides: Salt effects on ion pairs and hydrogen bonds, *Biochemistry 37*, 33−40.
20. Brandts, J. R., and Kaplan, K. J. (1973) Derivative spectroscopy applied to tyrosyl chromophores. Studies on ribonuclease, lima bean inhibitor, and pancreatic trypsin inhibitor, *Biochemistry 12*, 470−476.
21. Chen, Y. H., Yang, J. T., and Chau, K. H. (1974) Determination of helix and β-form of proteins in aqueous solution by circular-dichroism, *Biochemistry 13*, 3350−3359.
22. Lifson, S. (1961) Theory of Helix-Coil Transition in Polypeptides, *J. Chem. Phys. 34*, 1963−1975.
23. Doig, A. J. (2002) Recent advances in helix-coil theory, *Biophys. Chem. 101*, 281−293.
24. Stapley, B. J., Rohl, C. A., and Doig, A. J. (1995) Addition of side-chain interactions to modified Lifson-Roig helix-coil theory: Application to energetics of phenylalanine-methionine interactions, *Protein Sci. 4*, 2383−2391.
25. Rohl, C. A., Chakrabartty, A., and Baldwin, R. L. (1996) Helix propagation and N-cap propensities of the amino acids measured in alanine-based peptides in 40 volume percent trifluoroethanol, *Protein Sci. 5*, 2623−2637.
26. Brenner, S. E., Koehl, P., and Levitt, R. (2000) The ASTRAL compendium for protein structure and sequence analysis, *Nucleic Acids Res. 28*, 254−256.
27. Smith, D. (1989) *SSTRUC: A program to calculate a secondary structural summary*, Department of Crystallography, Birkbeck College, University of London, London.
28. Penel, S., Hughes, E., and Doig, A. J. (1999) Side-chain structures in the first turn of the α-helix, *J. Mol. Biol. 287*, 127−143.
29. Cochran, D. A. E., Penel, S., and Doig, A. J. (2001) Effect of the N1 residue on the stability of the α-helix for all 20 amino acids, *Protein Sci. 10*, 463−470.
30. Cochran, D. A. E., and Doig, A. J. (2001) Effect of the N2 residue on the stability of the α-helix for all 20 amino acids, *Protein Sci. 10*, 1305−1311.
31. Iqbalsyah, T. M., and Doig, A. J. (2004) Effect of the N3 residue on the stability of the α-helix, *Protein Sci. 13*, 32−39.
32. Chakrabartty, A., Kortemme, T., Padmanabhan, S., and Baldwin, R. L. (1993) Aromatic side-chain contribution to far-ultraviolet circular dichroism of helical peptides and its effect on measurement of helix propensities, *Biochemistry 32*, 5560−5565.
33. Doig, A. J., Chakrabartty, A., Klingler, T. M., and Baldwin, R. L. (1994) Determination of free energies of N-capping in α-helices by modification of the Lifson-Roig helix-coil theory to include N- and C-capping, *Biochemistry 33*, 3396−3403.
34. Scholtz, J. M., Qian, H., Robbins, V. H., and Baldwin, R. L. (1993) The energetics of ion-pair and hydrogen-bonding interactions in a helical peptide, *Biochemistry 32*, 9668−9676.
35. Nozaki, Y., and Tanford, C. (1967) Intrinsic dissociation constants of aspartyl and glutamyl carboxyl groups, *J. Biol. Chem. 242*, 4731−4735.

BI0508690